15th Australasian Fluid Mechanics Conference
The University of Sydney, Sydney, Australia
13-17 December 2004

Numerical Study of Moist Air Flow through the Ludwieg Tube

M. Tanaka[1], S. Matsuo[1], R. Nishizaki[1], H.D. Kim[2] and T. Setoguchi[1]

[1]Departmtnet of Mechanical Engineering
Saga University, 1 Honjo-machi, Saga, 840-8502 JAPAN

[2]School of Mechanical Engineering, Departmtnet of Mechanical Engineering
Andong National University, Songchun-dong, Andong, 760-749 Korea.

Abstract

A rapid expansion of moist air or steam in a supersonic nozzle gives rise to non-equilibrium condensation. If the latent heat released by condensation exceeds a certain quantity, the flow becomes unstable and a periodic flow oscillation occurs. In the present study, a numerical simulation of moist air flows in a supersonic nozzle was carried out using a special short duration supersonic wind tunnel, called a Ludwieg tube. In cases of nozzles with large throat height, the effects of initial relative humidity of the moist air on the flow field have been shown numerically. As a result, it was found that the characteristics of flow with occurrence of condensation were grouped into three types.

Introduction

A short duration supersonic wind tunnel, called a Ludwieg tube (or a Tube wind tunnel) [1,2], is recently receiving a renewed interest in simulating a space transportation system [3,4], because it is easy to achieve high Mach number and Reynolds numbers with relatively low turbulence, compared with the conventional supersonic and hypersonic wind tunnels. However the short duration of steady flow makes the flow measurements in the Ludwieg tube extremely difficult.

Typical example of a supersonic flow with heat addition is often found in Laval nozzle with a non-equilibrium condensation of moist air or steam, which is rapidly expanded through the nozzle (homogeneous nucleation) [5,6,7]. According to some previous works, the non-equilibrium condensation of moist air results in considerable total pressure losses [8]. In general, the process of heat addition almost always leads to unsteady wave motions even in a supersonic flow field [9,10,11].

In heterogeneous condensation [12], the condensation of the vapor takes place on foreign nuclei ; smoke and vapor from fires and various industries, dust from land surfaces, salt from oceans and particulate products from chemical reaction. Their presence in sufficient numbers leads to condensation near equilibrium at degree of supersaturation only slightly larger than unity.

Ludwieg tube has long been used to investigate the process of heat addition due to the condensation in the nozzle, since it provides well controlled flow conditions that permit operation with increased initial relative humidity and pressures [9,10]. From some previous researches, it was observed that the non-equilibrium condensation of moist air in a nozzle could lead to total pressure losses and flow instabilities as well [13]. However, detailed flow information with regard to time-dependent condensation in case of occurrence of condensation upstream of nozzle is not yet well known, since it is hard to reveal through experiments.

In the present study, a computational fluid dynamics work is applied to predict the condensation phenomena in the Ludwieg tube. The Ludwieg tube with a diaphragm downstream is simulated using the two-dimensional Navier-Stokes equations. In cases of nozzles with large throat height (case with occurrence of condensation upstream of nozzle), the effects of initial relative humidity of the moist air on the flow field have been shown numerically.

Computational analysis

Governing Equations

For simplicity of the present computational analysis, several assumptions are made; there is no velocity slip and no temperature difference between condensate particles and medium gas flows, and thus the energy relaxation processes between two phases are not considered in the present analysis. Due to very small condensate particles, the effect of the particles on pressure field of flow can be neglected.

The governing equations are unsteady, two - dimensional, compressible, Navier-Stokes equations and a droplet growth equation [14]. The equations described for compressible viscous flow were discretized by the finite difference method. Third-order TVD finite difference scheme [15] with MUSCL approach was used for spatial derivative terms and second-order central difference scheme in discretizing viscous terms. The spatially discretized equations are intergrated in time by means of a time splitting method that has the second order accuracy.

Baldwin-Lomax turbulence model is employed to close the governing equations [16]. The governing equations are mapped from the physical plane into a computational plane of a general transform and non-dimensionalized using the reference values at the initial conditions upstream of the nozzle.

Initial and Boundary Conditions

Computational grids of the Ludwieg tube flow field for the present computational analysis is schematically shown in figure 1, which was also used for the previous experimental work by Matsuo et al. [17]. The number of grids is 300×60. The Ludwieg tube consists of the upstream high-pressure tube, the convergent-divergent nozzle, and the downstream low-pressure tube. The Ludwieg tube has a length of 1000 mm. A diaphragm is located at the origin(x = 0) downstream of the nozzle throat, and separates the high and low-pressure tubes. The high and low-pressure tubes have the same height of H=38 mm. The convergent-divergent nozzle with a throat height of h^* (= 24 mm, 27 mm, 30 mm) is located at x = 302.5 mm upstream of the diaphragm and is in the shape of circular arcs with the same curvature radius of R^*=155 mm.

The pressures in the high and low-pressure tubes are defined as p_4 and p_1, respectively. In the present study, p_4 is kept constant at 101.3 kPa and the ratio of p_4 / p_1 (= p_{41}) is 5.0. The initial flow conditions in the high-pressure tube are given by pressure p_4, relative humidity φ_4 and temperature T_4. In the present computations, T_4 (=T_1) is kept constant at 302 K. The initial relative humidity φ_4 is set at 0 %, 20 %, 40 %, 60 % and 80 %.

Moist air is used as the working gas and assumed to be thermally

and calorically perfect. Inlet and outlet boundaries are constrained to the free boundary conditions. No velocity slip wall is assumed on adiabatic wall condition. Furthermore, condensate mass fraction $g = 0$ is given at the solid walls.

Results and Discussions

Figures 2, 3 and 4 show the time-dependent characteristics of static pressure p on the centre line of the Ludwieg tube in cases of $\varphi_4 = 20$ %, 40 % and 80 %, respectively. The height of the nozzle throat in each figure is 27 mm. The abscissa is the distance x measured from the diaphragm divided by the tube height H. t in figures 2(a), 3(a) and 4(a) is the elapsed time after the rupture of diaphragm. Broken lines in figures 2(b), 3(b) and 4(b) denote the distribution of the static pressure for $\varphi_4 = 0$ %.

As seen from figure 2, variations of the static pressure p are found in the region close to the nozzle throat and at slightly upstream part of nozzle. In this case, a condensation shock wave builds up periodically in the divergent nozzle section and it moves upstream through the throat [18]. This corresponds to the case of Type A in Table 1 as described later. The pressure variation is due to the periodic excursions of the condensation shock wave. The variation of p for $\varphi_4 = 40$ % (figure 3) is similar to that for $\varphi_4 = 20$ % (figure 2).

In figure 4 ($\varphi_4 = 80$ %), variations of the static pressure are not found in the region upstream of the nozzle throat. Furthermore, in

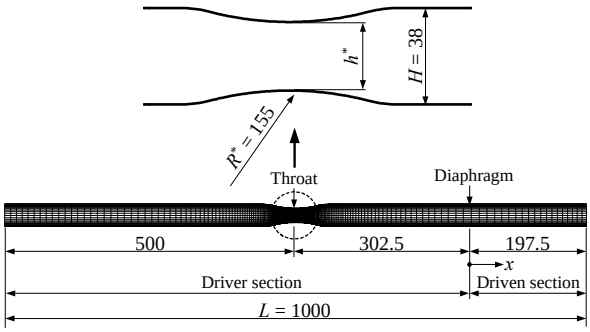

Figure 1. Computational grids (Unit : mm).

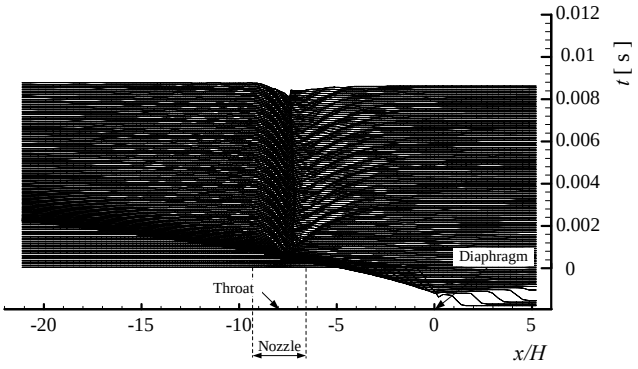

(a) Wave diagram.

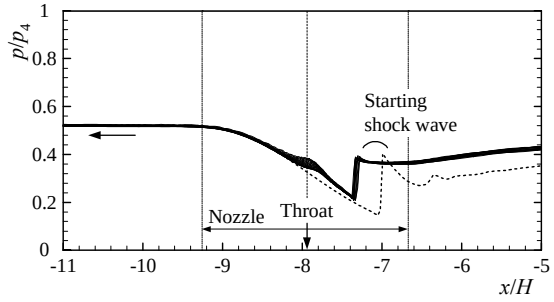

(b) Distributions of static pressure (t = 7.86 ~ 9.45 μs).

Figure 2. Time dependent distributions of static pressure (h^* = 27 mm, φ_4 = 20 %).

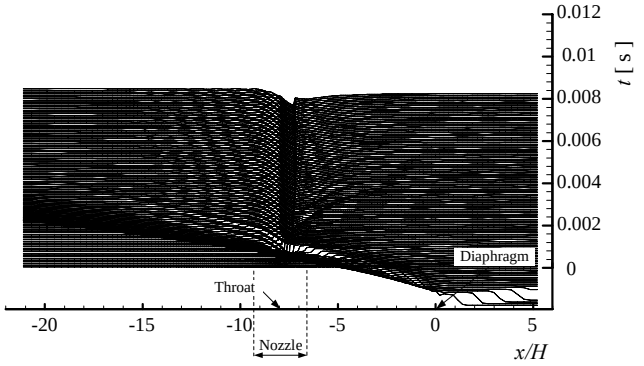

(a) Wave diagram.

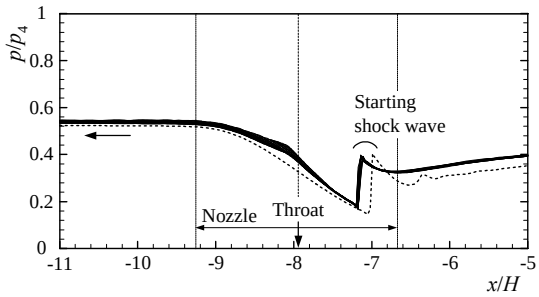

(b) Distributions of static pressure (t = 7.87 ~ 9.43 μs).

Figure 3. Time dependent distributions of static pressure (h^* = 27 mm, φ_4 = 40 %).

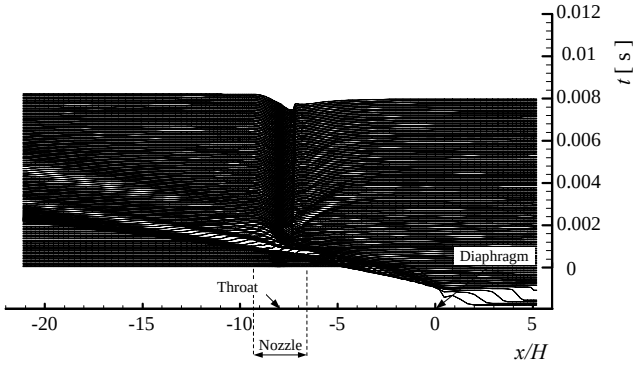

(a) Wave diagram.

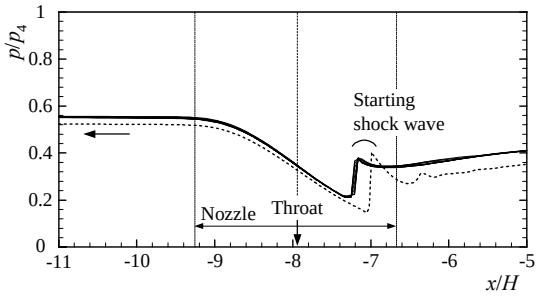

(b) Distributions of static pressure (t = 7.84 ~ 9.42 μs).

Figure 4. Time dependent distributions of static pressure (h^* = 27 mm, φ_4 = 80 %).

this region it is found that the static pressure value (solid lines in figures 3 and 4) is larger than that (broken lines) for φ_4 = 0 %. This is due to the latent heat released by the non-equilibrium condensation. The variation of p for φ_4 = 60 % was similar to that for φ_4 = 80 % (figure 4).

Figures 5, 6 and 7 show the time-dependent characteristics (x - t diagram) of nucleation rate I (number of condensate nuclei per unit time and unit volume) and g (ratio of the condensate mass fraction to total mass flow through the Ludwieg tube) on the centre line for φ_4 =20 %, 40 % and φ_4 =80 %, respectively (h*= 27 mm). Each line in these figures indicates the time increment of about 0.08 μs. As seen from figure 5(a) (φ_4 = 20 %), the nucleation rate and condensate mass fraction start to increase rapidly at the position close to the nozzle throat. Furthermore, the condensate nuclei (nucleation rate) are not found in the region upstream of the nozzle.

In figure 6 (φ_4 = 40 %), the condensate nuclei seem to generate mainly in the region close to the nozzle throat and it is found even upstream of the nozzle periodically. The variation of g in the region close to the nozzle throat is larger than that in figure 5(b) and a larger amount of droplets are generated in that region. But it was not seen upstream of the nozzle.

In figure 7(a), the spatial distribution of the condensate nuclei seems to be of a narrow zone with a sharp peak and a large number of the condensate nuclei is generated even upstream of the nozzle as the time proceeds. The condensate mass fraction is seen in the whole region in contrast to the case of that in figures 5 and 6 (figure 7(b)). Furthermore, occurrence of the condensate mass fraction in the region upstream of the nozzle in figure 7(b) is due to that of the condensate nuclei in this region. The change of I and g for φ_4 = 60 % was similar to that for φ_4 = 80 %.

Table 1 shows the classification of the flow field with non-equilibrium condensation obtained by the present simulations.

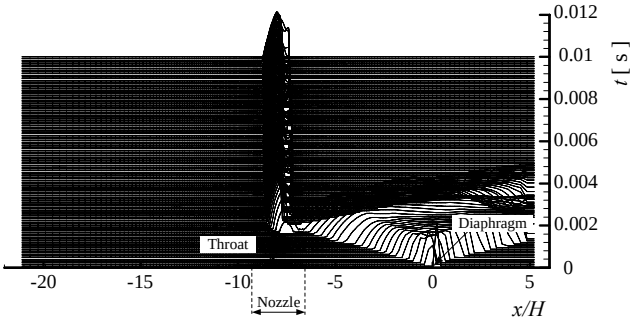

(a) Nucleation rate.

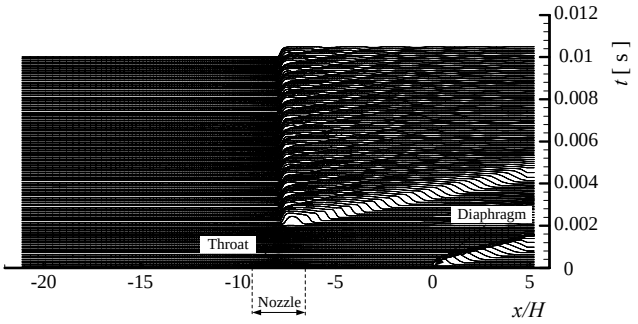

(b) Condensate mass fraction.

Figure 5. Time dependent distributions of condensate mass fraction and nucleation rate (h^* = 27 mm, φ_4 = 20 %).

From the point of view of occurrence of condensate nuclei and condensate mass fraction, and variation of the static pressure, there are three kinds of flow field with non-equilibrium condensation as follows :

A : At the upstream part of the nozzle, variations of the static pressure are slightly found. But occurrence of the condensate mass fraction and nucleus are not recognized. In the region of the nozzle throat, occurrence of the condensate mass fraction

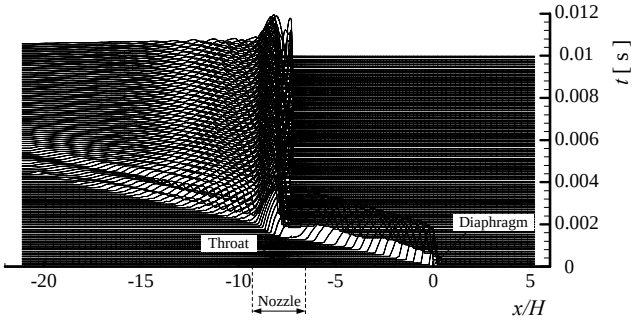

(a) Nucleation rate.

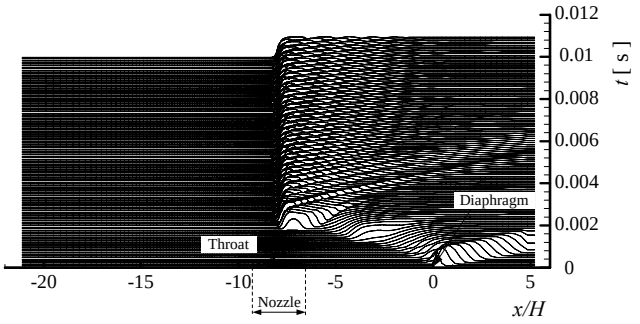

(b) Condensate mass fraction.

Figure 6. Time dependent distributions of condensate mass fraction and nucleation rate (h^* = 27 mm, φ_4 = 40 %).

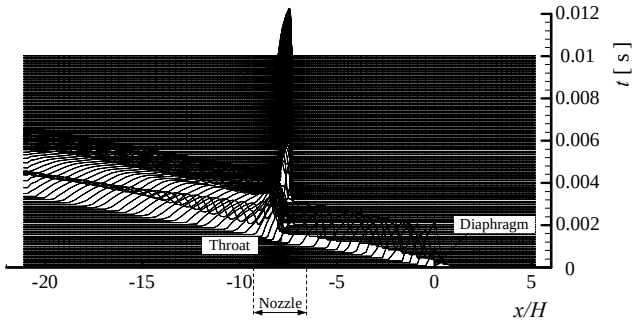

(a) Nucleation rate.

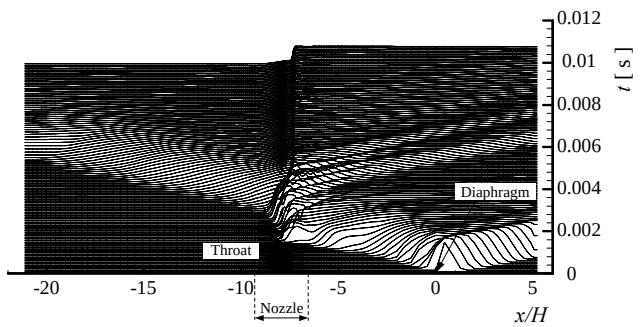

(b) Condensate mass fraction.

Figure 7. Time dependent distributions of condensate mass fraction and nucleation rate (h^* = 27 mm, φ_4 = 80 %).

and the nucleus, and variation of the static pressure are recognized.

B : At the upstream part of the nozzle, variations of the static pressure and occurrence of the nucleus are found. But occurrence of the condensate mass fraction are not found. In the region close to the nozzle throat, occurrence of the condensate mass fraction and the nucleus, and variation of the static pressure are recognized.

C : At the upstream part of the nozzle, variations of the static pressure are not found. Occurrence of the nucleus and the condensate mass fraction are found in this region.

As seen from Table 1, the flow field for case with large nozzle height is different from that (Type A) obtained from the previous researches [13].

Figure 8 shows a time dependent characteristics of *p-T* diagram for φ_4 = 20 %, 40 %, 60 % and 80 % (h^*= 27 mm). Solid line in this figure is a liquid-vapour saturation line. Each line denotes the variation of pressure and temperature of vapour at the position close to the maximum degree of supersaturation. As seen from this figure, the variation of vapour pressure and temperature becomes very complicated as time proceeds and the line for φ_4 = 80 % approaches the saturation line as time proceeds in contrast to the cases of φ_4 = 40 % and 60 %. This means that the condensation proceeds heterogeneously and the relative position between a liquid – vapour saturation line and the position after time proceed does not depend on the value of initial relative humidity in driver section. The time-dependent variations of the line for Type C in Table 1 showed almost as the same tendency as that in figure 8.

Conclusions

In order to investigate the time-dependent behavior of condensation of moist air through the Ludwieg tube, a computational fluid dynamics work was applied to the two - dimensional, compressible, Navier - Stokes equations, fully coupled with the droplet growth equations. As a result, it was found that the height of the nozzle throat strongly effected the occurrence of condensation in the Ludwieg tube and from the point of view of occurrence of nuclei and condensate mass fraction, and variation of the static pressure, three kinds of flow field with non-equilibrium condensation were obtained by the present simulations.

		φ (%)			
		20	40	60	80
h^* (mm)	24	A	A	B	C
	27	A	B	C	C
	30	B	C	C	C

Table 1. Classification of flow with condensation.

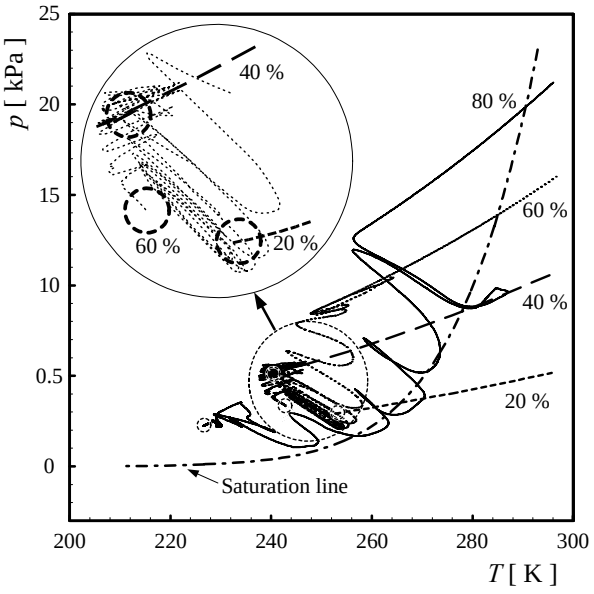

Figure 8. *p-T* diagram (h^* = 27 mm).

References

[1] Ludwieg, H., Der Rohrwindkanal, *Zeitschrift für Flugwissenschaften*, **3(7)**, 1955, 206-216.

[2] Cable, A. J. & Cox, R. N., The Ludwieg pressure tube supersonic wind tunnel, *The AeronauticalQuarterly*, **14(2)**, 1963, 143-157.

[3] Friehmelt, H., Koppenwaller, G. & Müller-Eigner, R., Calibration and first results of a redesigned Ludwieg expansion tube, *AIAA/DGLR Fifth International Aerospace Planes and Hypersonics Technologies Conference*, AIAA-**93(5001)**, 1993.

[4] Schneider, S. P. & Haven, C. E., Quiet-Flow Ludwieg Tube for High-Speed Transition Research, *AIAA J.*, **33(4)**, 1995, 688-693.

[5] Wegener, P. P. & Mack, L.M., Condensation in supersonic hypersonic wind tunnels, *Adv. In Appl. Mech.*, **5**, Academic Press, 1958.

[6] Matsuo, K., Kawagoe, S., Sonoda, K. & Sakao, K., Studies of Condensation Shock Waves (part 1, Mechanism of their Formation), *Bulletin of JSME*, **28**, 1985, 2577-2582.

[7] Schnerr, G. H, Homogene Kondensation in Sationären Transsonischen Strömungen durch Lavaldüsen und um Profile, Habilitationsschrift, Universität Karlsruhe (TH), Germany, 1986.

[8] Kwon, S. B., Matsuo, K., Kawagoe, S. & Matsuo, S., Total Pressure Loss in Supersonic Nozzle Flows with Condensation, *JSME Int. J.*, **31(1)**, 1988, 16-21.

[9] Wegener, P. P. & Cagliostro, D. J., Periodic nozzle flow with heat addition, *Combustion Sci. and Tech.*, **6**, 1973, 269-277.

[10] Matsuo K, Kawagoe S, Sonoda K and Setoguchi T. Oscillations of Laval nozzle flow with condensation (part 1), *Bulletin of JSME*, **28(241)**, 1985, 1416-1422.

[11] Adam, S. & Schnerr, G. H., Instabilities and bifurcation of non-equilibrium two-phase flows, *J. Fluid Mech.*, **348**, 1997, 1-28.

[12] Wegener, P. P., *Nonequilibrium Flow*, Part 1, Marcel Dekker, 1969.

[13] Matsuo, S., Tanaka, M., Setoguchi, T. & Kim, H. D., Numerical Visualization of Moist Air Flow through the Ludwieg Tube, *Proc. of the 13th Int. Symposium on Transport Phenomena*, 2002, 151-156.

[14] Sislian, J. P., Condensation of water vapour with or without a carrier gas in a shock tube, *UTIAS Report* **201**, 1975.

[15] Yee, H. C., A class of high-resolution explicit and implicit shock-capturing methods, *NASA TM*-**89464**, 1989.

[16] Baldwin, B.S. & Lomax, H., Thin layer approximation and algebraic model for separated turbulent flows, *AIAA Paper. No.***78-257**, 1978.

[17] Matsuo, K., Kawagoe, S., Sonoda, K. & Setoguchi, T., Oscillations of Laval nozzle flow with condensation (part 1, on the range of oscillations and their frequencies), *Bulletin of JSME*, **26(219)**, 1983, 1556-1562.

[18] Setoguchi, T., Matsuo, S., Shimamoto, K., Yasugi,S. & Yu, S., Passive control of unsteady condensation shock wave, *J. of Thermal Science,* **9(4)**, 2000, 299-304.